PHYSICAL REVIEW B **80**, 121308(R) (2009)

Electric field tuning of spin-orbit coupling in $KTaO_3$ field-effect transistors

H. Nakamura and T. Kimura

Division of Materials Physics, Graduate School of Engineering Science, Osaka University, Toyonaka, Osaka 560-8531, Japan

(Received 9 September 2009; published 28 September 2009)

We report on the observation of weak antilocalization associated with large spin-orbit coupling in a tunable *d* electron system: a quasi-two-dimensional electron gas formed in a $KTaO_3$ field-effect transistor. We find that spin-precession length of electrons can be tuned by gate voltage V_G and is as short as tens of nanometers at large V_G. Our results show that 5*d* transition-metal compounds having strong atomic spin-orbit couplings induced by heavy 5*d* elements could be utilized to electrically manipulate spins in nanoscale spintronic devices.

DOI: 10.1103/PhysRevB.80.121308 PACS number(s): 85.75.−d, 73.20.Fz, 73.40.Qv

Spin-orbit coupling is a key ingredient in a number of proposed future spintronic devices, because it relates spin of an electron to its motion, providing a way to control spins electrically.[1,2] A prerequisite for spin-orbit coupling is the electric field orthogonal to an electron motion: the coulomb potential of atoms leads to an atomic spin-orbit coupling, whereas in a solid more macroscopic electric fields can have a significant effect. Among the latter type, Rashba spin-orbit coupling,[3] induced by the inversion asymmetry of potential wells, offers a unique possibility to control spins by external electric fields.[4] The Rashba effect has been studied in a number of systems including semiconductors[4–13] and metal surfaces.[14] However, the gate control of the Rashba effect has so far been demonstrated exclusively in III-V or II-VI type semiconductors.[4,7–13] In these materials, the lack of inversion symmetry in the bulk crystals leads to another spin-orbit coupling called the Dresselhaus term, which in general makes the interpretation more complicated.[15] Thus, exploring different systems that enable gate control of the Rashba effect would be valuable to understand basic physics as well as to design useful spintronic devices.

Our target material in the present study is a cubic perovskite oxide, $KTaO_3$, which is known to be a wide gap insulating oxide ($E_g \sim 3.5$ eV), displaying quantum paraelectricity[16] and high mobility *n*-type conduction with doping.[17] A field-effect-transistor operation has also been observed in $KTaO_3$ around room temperature.[18] These features are common with $SrTiO_3$, another perovskite acquiring much recent interest as a component of complex oxide heterostructures.[19] These two perovskite oxides, however, differ in the strength of (microscopic) spin-orbit interaction, which is much enhanced in $KTaO_3$ containing a heavy 5*d* element, tantalum. Figure 1(a) shows a schematic band structure of $KTaO_3$. Conduction bands originating from triply degenerate t_{2g} electronic states of 5*d* electrons[20] are split by the spin-orbit interaction into the lower doubly degenerate bands [the light-electron (LE) band and the heavy-electron (HE) band][21] and the higher spin-orbit (SO) split band.[22] For $KTaO_3$, the magnitude of the splitting Δ_{SO}, which is a measure of the strength of atomic spin-orbit coupling, is 400 meV (Ref. 22) and is by more than an order of magnitude larger than that for $SrTiO_3$ ($\sim$17 meV).[23] In this Rapid Communication, we show that this large microscopic spin-orbit coupling in $KTaO_3$, when incorporated in a field-effect transistor (FET), can be used to induce tunable spin-orbit fields on electrons.

We fabricated FET structures on top of $KTaO_3$ single crystals, as illustrated in the left inset of Fig. 1(b). The step-and-terrace structures, indicating the atomic flatness of the $KTaO_3$ (100) surfaces, were observed by atomic force microscopy. First, 20 nm thick aluminum contacts with Hall bar geometry were evaporated on the surface. Next, parylene insulator (ε_r=3.15) with thickness of around 0.3 μm was coated to serve as a gate insulator. Finally, 30-nm-thick gold contacts were patterned on top of the parylene for gate electrodes. Channel area was 400 μm in length and 200 μm in width. Details of the device fabrication process were reported previously for a similar device with $SrTiO_3$ channel.[24] Standard dc four-probe method was used to measure the sheet resistance R_{2D} of the channel. Gate leak current did not exceed 5 nA and was at all times less than the channel current by more than two orders of magnitudes. Temperature and magnetic field controls were obtained by a cryostat

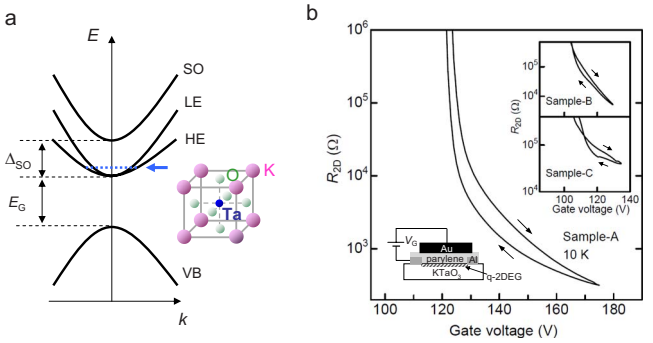

FIG. 1. (Color online) (a) Schematic band structure of $KTaO_3$. The conduction band consists of HE, LE, and SO split bands, originating from the empty Ta 5*d* states (Refs. 20–22). Spin-orbit induced splitting Δ_{SO} of these bands is 0.4 eV (Ref. 22). The valence band is mainly made up of O 2*p* states strongly hybridized by Ta 5*d* states (Ref. 20). The thick blue arrow indicates the approximate position of the Fermi level of quasi-two-dimensional electron gas induced in $KTaO_3$-FETs. Note that the expected splitting of HE and LE bands due to the confinement of carriers is neglected in this figure. (b) Sheet resistance R_{2D} versus gate voltage V_G measured at 10 K for three samples. Each sample differed in parylene thickness: 0.39 μm (sample A), 0.34 μm (sample B), and 0.37 μm (sample C). Gate sweep rate was 0.1 V/s. The left inset shows a schematic device structure.

equipped with an 8 T superconducting magnet (Oxford Instruments).

Figure 1(b) shows field-effect characteristics of $KTaO_3$ FETs at 10 K for three samples with different parylene thickness: 0.39, 0.34, and 0.37 μm, for samples A–C, respectively. Although the $KTaO_3$ channels were highly resistive ($>G\Omega$) in the absence of gate voltage V_G, they became conducting by applying large V_G of over 100 V, where reversible modulation of sheet resistance R_{2D} was observed for all of the three samples. The most prominent field effect was observed in sample A, where R_{2D} reached about 800 Ω at large V_G. These results show that a large positive gate voltage induces substantial electron accumulation at the parylene/$KTaO_3$ interface. The hystereses observed in the R_{2D}-V_G curves probably reflect trap and release of mobile electrons at traps. The Hall measurements were carried out for sample A at 10 K, which gave sheet carrier density $n_{2D}=2.67\times10^{12}$ cm^{-2} at $V_G=155$ V. This value roughly represents a maximum sheet carrier density achieved in sample A. The corresponding Hall mobility μ_H at the same gate voltage was 2600 cm^2/V s, higher than in a parylene/$SrTiO_3$ FET reported previously.[24] This is consistent with the smaller effective mass of electrons in $KTaO_3$.[21] The Shubnikov–de Haas (SdH) oscillation was not observed at magnetic fields B below 8 T and temperatures T above 2 K in our samples, probably due to the still insufficient mobilities.

We adopted weak antilocalization[25,26] as a probe of spin-orbit coupling in the parylene/$KTaO_3$-FETs. Weak localization (WL) and weak antilocalization (WAL) are fundamentally quantum interference phenomena of electrons. At sufficiently low T, constructive interferences of electron waves lead to the enhanced probability of back scattering events, resulting in an extra resistivity added to the classical value (weak localization). When spin-orbit coupling allow the electron spin to flip, however, the constructive interference changes sign to the destructive one, resulting in a decreased resistivity (antilocalization).[26] Both effects are destroyed by applying B, thus yielding negative (positive) magnetoresistance for weak localization (antilocalization). Therefore, WAL can be a sensitive probe of spin-orbit coupling. WAL has so far been used to detect spin-orbit coupling in systems ranging from metals,[25] semiconductors,[6–12] to graphene.[27]

Figure 2(a) shows magnetoresistance (MR) data at 2.4 K at three different gate voltages for sample A. Magnetic fields were applied perpendicular to the plane of the parylene/$KTaO_3$ interface. A clear positive MR is seen in low B region at all the gate voltages. This positive MR was only observed in the configuration of B normal to the interface, and is a signature of WAL which reflects the presence of spin-orbit coupling in the system.[25,26] It can be seen that a broad negative MR (weak localization) is superimposed on the sharp positive MR at $V_G=145$ V, while only the positive MR is observable at $V_G>150$ V. This suggests that the spin-orbit coupling in our system is exceptionally strong at larger V_G.[25] At $V_G=160$ V, a broader positive MR proportional to B^2 is visible in addition to the sharp antilocalization dip. This is a classical MR caused by the Lorentz force acting on conduction electrons when more than two types of carriers are present.[28] It is worth mentioning that the sharp positive MR

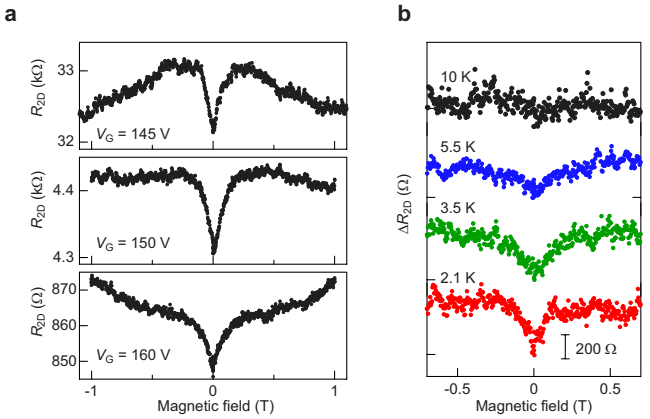

FIG. 2. (Color online) (a) Magnetoresistance of sample A at 2.4 K measured at gate voltages of 145, 150, and 160 V. Magnetic fields were applied normal to the plane of the parylene/$KTaO_3$ interface. Small backgrounds caused by residual relaxation are subtracted from the data. (b) Isothermal magnetoresistance $\Delta R_{2D}=R_{2D}(B)$-$R_{2D}(0)$ for sample C at $V_G=127$ V taken at several temperatures. $R_{2D}(0)$ was in the range 21–24 kΩ for temperatures between 2.1 and 10 K.

due to antilocalization has not been observed in chemically doped $KTaO_3$ crystals[29] nor in FETs based on $SrTiO_3$ at the similar temperature and sheet resistance range.[30] Temperature dependent measurements [Fig. 2(b)] at a constant gate voltage showed that the WAL dip was suppressed as the temperature was raised to about 10 K.

We now compare our result with the theory of Iordanskii, Lyanda-Geller, and Pikus (ILP theory),[31] developed to describe WAL including the contribution of Rashba-type spin-orbit coupling. The theory was derived for the diffusive regime, i.e., $B<B_{tr}=\hbar/2el_m^2$, where B_{tr} is the transport field characterizing elastic scattering of electrons, $\hbar$ is the Planck's constant, e is the electron charge, and l_m is the mean-free path. In our samples, we estimate $B_{tr}>0.1$ T. Although this model includes spin-dependent energy splitting of electrons proportional to both k and k^3,[6] where k is the electron wave vector, better fits were obtained by neglecting terms linear in k.[32] In this condition, the theory involves two fitting parameters: B_ϕ and B_{SO}, the magnetic fields characterizing the phase coherence length and the spin-precession length, respectively. The best fits to the data of samples A and B obtained by adjusting these parameters are shown in Fig. 3. Here, the vertical axes show sheet conductance change $\Delta\sigma$ in applied B, where $\sigma=1/R_{2D}$, in units of $e^2/\pi h$. The observed WAL peaks are well reproduced by the theory, suggesting that the essential physics is captured by the ILP theory. It should be noted that, although in a strict sense ILP theory is valid only in a diffusive regime, agreement between the fitting curves and the experimental MR curves in a wider B range ($B<0.2$–0.3 T) was taken into account. It has been shown that this approach gives better agreement between B_{SO} estimated by WAL and that by beating of SdH oscillations.[12]

The parameters B_ϕ and B_{SO} are related to the characteristic length scale l by $B=\hbar/4el^2$. Using this relation, we obtained V_G dependence of the phase coherence length l_ϕ and

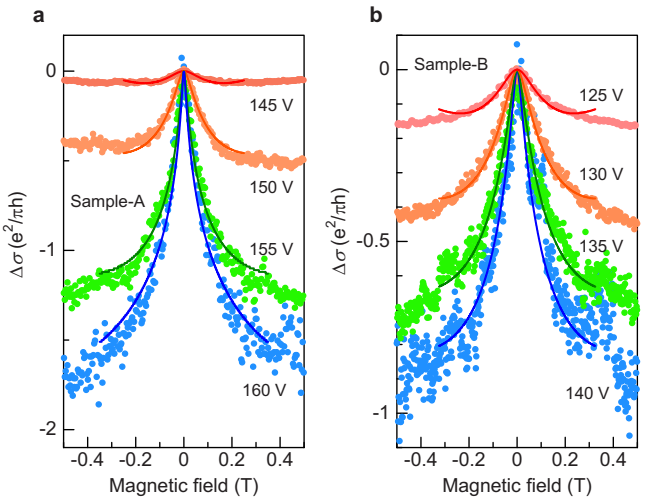

FIG. 3. (Color online) Experimental magnetoconductance $\Delta\sigma = \sigma(B) - \sigma(0)$ (dots), in units of $e^2/\pi h$, along with the best theoretical fits (solid curves) to the data obtained by the ILP theory (see text). (a) Results for Sample-A at 2.4 K for V_G of 145–160 V. $R_{2D}(B=0)$ at each V_G was 32.1 (145), 4.30 (150), 1.53 (155), and 0.86 kΩ (160 V). (b) Results for sample B at 2.5 K for V_G of 125–140 V. $R_{2D}(B=0)$ at each V_G was 21.1 (125), 5.74 (130), 2.70 (135), and 1.43 kΩ (140 V).

the spin-precession length l_{SO}. The results are shown in Fig. 4. It can be seen that l_ϕ, which is about 0.25 μm at 160 V for sample A, decreases monotonically to 0.07 μm at 145 V (inset of Fig. 4). The same trend is seen for sample B. This indicates that electrons rapidly lose phase coherence as the insulating regime is approached from the conducting side.[33] The spin-precession length l_{SO}, on the other hand, decreases as V_G is increased, from 60 nm at 145 V to 20 nm at 160 V (sample A). This threefold change in l_{SO} tuned by gate voltage is remarkably large, and is comparable to a recent observation in a GaInAs/InP heterostructure:[10] obviously this is due to the large carrier tunability obtained in both systems. We also note that l_{SO} of around 20 nm obtained under large V_G is exceptionally small. [e.g., $l_{SO} > 100$ nm in n-type III-V semiconductor heterostructures for strong spin-orbit coupling conditions;[9,10] for p-type structures, $l_{SO} > 200$ nm (Ref. 34)].

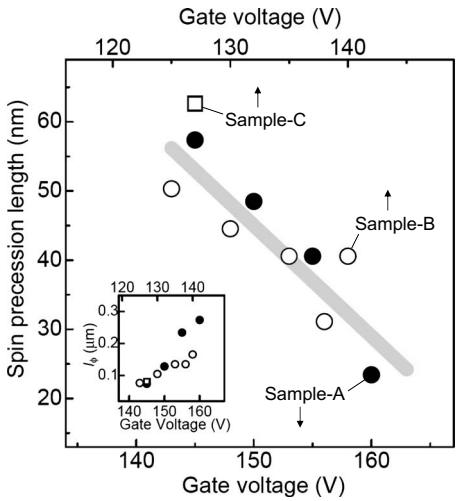

FIG. 4. The spin-precession length l_{SO}, plotted against the gate voltage for samples A–C. Data for samples A–C were taken at 2.4, 2.5, and 2.1K, respectively. The bold gray line is a guide to the eyes. The inset shows the phase coherence length l_ϕ versus gate voltage for samples A (filled circle), B (open circle), and C (open square). The gate voltage for sample A (B and C) is shown in the bottom (top) axis.

The unusually short spin-precession length observed in $KTaO_3$-FETs originates from strong spin-orbit coupling, combined with the large effective mass of electrons (~1 for heavy-electron mass[21]). Since $l_{SO} = \sqrt{D\tau_{SO}}$, where D is the diffusion constant and τ_{SO} is the spin-precession time, large effective mass and strong spin-orbit coupling contribute to small D and τ_{SO}, respectively, leading to short l_{SO}. [Note that introducing more defects in other semiconductors and making just their mobility low could not in general result in short l_{SO} because this would cause larger τ_{SO}.[1]) These features make $KTaO_3$-FET unique among many other conventional semiconductor structures, and seem attracting to realize spintronic devices such as spin-FETs (Ref. 1) with a nanoscale channel length.

It is intriguing to consider the origin of strong spin-orbit coupling probed at $KTaO_3$ interfaces. We first note that the impurity mechanism (caused by unintentionally doped heavy impurity atoms) can be ruled out because recent work on photocarrier-doped bulk $KTaO_3$ revealed the absence of WAL even under the condition that negative MR due to WL was observed[35] (see Ref. 36 for related work on $SrTiO_3$). Second, although the bulk inversion asymmetry (BIA) of an underlying crystal structure could also lead to spin-orbit coupling, this contribution should be small in $KTaO_3$ where all the atoms occupy centers of inversion (though not totally ruled out because applied electric field may induce nonzero BIA due to the almost-ferroelectric nature of $KTaO_3$). Thus, the most robust mechanism of spin-orbit coupling for the present system is the Rashba effect, originating from the inversion asymmetry of the confining potential. Since both the macroscopic electric field and the microscopic spin-orbit interaction from the atomic cores contribute to the Rashba effect,[15] one can expect greatly enhanced effect for $KTaO_3$-FET containing a heavy $5d$ element.

In conclusion, we have demonstrated the gate control of spin precession in $KTaO_3$ field-effect transistors. The present system is distinct from more conventional III-V semiconductors in that carriers originate from d-orbitals having large electron mass, and in that underlying crystal structure possesses inversion symmetry. The latter means that the strong spin-orbit coupling observed in this system is most likely to originate solely from the Rashba effect. These features would provide a new opportunity to study spin-orbit coupling effects in solids.

We thank T. Koga and Y. Kozuka for valuable discussions, and T. Nozaki and K. Miyajima for their help in characterizing parylene films. This work was supported in part by KAKENHI (Grants No. 20840029, No. 20001004, and No. 20674005) and the Global COE Program (G10) of the Japan Society for the Promotion of Science.

[1] I. Zutic, J. Fabian, and S. D. Sarma, Rev. Mod. Phys. **76**, 323 (2004).
[2] D. D. Awschalom and M. E. Flatté, Nat. Phys. **3**, 153 (2007).
[3] Y. A. Bychkov and E. I. Rashba, JETP Lett. **39**, 78 (1984).
[4] J. Nitta, T. Akazaki, H. Takayanagi, and T. Enoki, Phys. Rev. Lett. **78**, 1335 (1997).
[5] P. D. Dresselhaus, C. M. A. Papavassiliou, R. G. Wheeler, and R. N. Sacks, Phys. Rev. Lett. **68**, 106 (1992).
[6] W. Knap *et al.*, Phys. Rev. B **53**, 3912 (1996).
[7] T. Koga, J. Nitta, T. Akazaki, and H. Takayanagi, Phys. Rev. Lett. **89**, 046801 (2002).
[8] J. B. Miller, D. M. Zumbuhl, C. M. Marcus, Y. B. Lyanda-Geller, D. Goldhaber-Gordon, K. Campman, and A. C. Gossard, Phys. Rev. Lett. **90**, 076807 (2003).
[9] N. Thillosen, S. Cabanas, N. Kaluza, V. A. Guzenko, H. Hardtdegen, and T. Schapers, Phys. Rev. B **73**, 241311(R) (2006).
[10] V. A. Guzenko, T. Schäpers, and H. Hardtdegen, Phys. Rev. B **76**, 165301 (2007).
[11] G. M. Minkov, A. A. Sherstobitov, A. V. Germanenko, O. E. Rut, V. A. Larionova, and B. N. Zvonkov, Phys. Rev. B **71**, 165312 (2005).
[12] B. Grbic, R. Leturcq, T. Ihn, K. Ensslin, D. Reuter, and A. D. Wieck, Phys. Rev. B **77**, 125312 (2008).
[13] X. C. Zhang, A. Pfeuffer-Jeschke, K. Ortner, V. Hock, H. Buhmann, C. R. Becker, and G. Landwehr, Phys. Rev. B **63**, 245305 (2001).
[14] S. LaShell, B. A. McDougall, and E. Jensen, Phys. Rev. Lett. **77**, 3419 (1996).
[15] R. Winkler, *Spin-orbit Coupling Effects in Two-Dimensional Electron and Hole Systems* (Springer, Berlin, 2003).
[16] K. A. Müller and H. Burkard, Phys. Rev. B **19**, 3593 (1979).
[17] S. H. Wemple, Phys. Rev. **137**, A1575 (1965).
[18] K. Ueno, I. H. Inoue, T. Yamada, H. Akoh, Y. Tokura, and H. Takagi, Appl. Phys. Lett. **84**, 3726 (2004).
[19] J. Mannhart, D. H. A. Blank, H. Y. Hwang, A. J. Millis, and J. M. Triscone, MRS Bull. **33**, 1027 (2008).
[20] T. Neumann, G. Borstel, C. Scharfschwerdt, and M. Neumann, Phys. Rev. B **46**, 10623 (1992).
[21] H. Uwe, J. Kinoshita, K. Yoshihiro, C. Yamanouchi, and T. Sakudo, Phys. Rev. B **19**, 3041 (1979).
[22] H. Uwe, K. Oka, H. Unoki, and T. Sakudo, J. Phys. Soc. Jpn. **49**, Suppl. A, 577 (1980).
[23] H. Uwe, T. Sakudo, and H. Yamaguchi, Jpn. J. Appl. Phys. **24**, Suppl. 24-2, 519 (1985).
[24] H. Nakamura, H. Takagi, I. H. Inoue, Y. Takahashi, T. Hasegawa, and Y. Tokura, Appl. Phys. Lett. **89**, 133504 (2006).
[25] G. Bergmann, Phys. Rep. **107**, 1 (1984).
[26] S. Hikami, A. I. Larkin, and Y. Nagaoka, Prog. Theor. Phys. **63**, 707 (1980).
[27] X. Wu, X. Li, Z. Song, C. Berger, and W. A. de Heer, Phys. Rev. Lett. **98**, 136801 (2007).
[28] N. W. Ashcroft and N. D. Mermin, *Solid State Physics* (Saunders, Philadelphia, 1981).
[29] W. R. Hosler and H. P. R. Frederikse, Solid State Commun. **7**, 1443 (1969).
[30] H. Nakamura, H. Tomita, H. Akimoto, R. Matsumura, I. H. Inoue, T. Hasegawa, K. Kono, Y. Tokura, and H. Takagi, J. Phys. Soc. Jpn. **78**, 083713 (2009).
[31] S. V. Iordanskii, Y. B. Lyanda-Geller, and G. E. Pikus, JETP Lett. **60**, 206 (1994).
[32] Note that Rashba effect leads to k^3 spin splitting, e.g., for GaAs hole band: angular momentum $j=3/2$ of the hole band gives rise to the higher order effect (Ref. 15). This argument can also be applied to the present system because the conduction-band minimum of $KTaO_3$ is analogous to the valence-band maximum of GaAs from the symmetry point of view (Ref. 37). When k^3 spin splitting is dominant, ILP theory gives the same result (Refs. 6 and 12) as the Hikami-Larkin-Nagaoka theory (Ref. 26).
[33] The phase breaking mechanism most relevant in the present condition is probably the small-energy-transfer electron-electron scattering, which leads to $l_\phi \propto T^{-0.5}$ (Ref. 38). We find $A=0.2-0.6$ (in $l_\phi \propto T^{-A}$) depending on the sample and the gate voltage: we think, however, that the T range (2–8 K) available for extracting A is insufficient to discuss the phase breaking mechanism.
[34] Estimated for structures studied in Refs. 11 and 12 using parameters therein.
[35] Y. Kozuka (private communication).
[36] Y. Kozuka, Y. Hikita, T. Susaki, and H. Y. Hwang, Phys. Rev. B **76**, 085129 (2007).
[37] L. F. Mattheiss, Phys. Rev. B **6**, 4718 (1972).
[38] J. J. Lin and J. P. Bird, J. Phys.: Condens. Matter **14**, R501 (2002).